energies

MDPI

Article

Temperature Field Simulation and Energy Analysis of a Heat Pump Tobacco Bulk Curing Barn

Ye Zhang [1], Bin Li [2], Zhenfeng He [1], Wenyan Ou [1], Jiahao Zhong [1], Xuefeng Zhang [1], Mingang Meng [1] and Changyou Li [1,*]

[1] College of Engineering, South China Agricultural University, Guangzhou 510642, China
[2] College of Intelligent and Manufacturing Engineering, Chongqing University of Arts and Sciences, Yongchuan, Chongqing 402160, China
* Correspondence: lichyx@scau.edu.cn; Tel.: +86-20-85280817

Abstract: Recently, heat pump drying has been widely used in tobacco processing. Considering the importance of this issue, it is of significant importance to further investigate temperature distribution and energy analysis in the drying process. To develop an energy-saving, environmental-friendly, and high-quality tobacco drying method, temperature distribution, dehumidification performance, the economic issues, and thermal efficiency of a heat pump curing barn (HPCB) and a traditional coal-fired bulk curing barn (TCCB) were compared. The regional temperature eigenvalue model was applied to describe the temperature uniformity with HPCB and TCCB. Moreover, thermal efficiency was obtained through energy tests. The obtained results showed that HPCB is beneficial to improve the drying quality of tobacco. The performed analyses showed that the thermal efficiency of the TCCB and HPCB was 42.02% and 66.53%, respectively. Accordingly, heat pump technology is recommended for industrial drying of tobacco leaves and obtaining high-quality products.

Keywords: tobacco bulk curing; heat pump; temperature field; moisture dehumidification rate; thermal efficiency

Citation: Zhang, Y.; Li, B.; He, Z.; Ou, W.; Zhong, J.; Zhang, X.; Meng, M.; Li, C. Temperature Field Simulation and Energy Analysis of a Heat Pump Tobacco Bulk Curing Barn. *Energies* **2022**, *15*, 8655. https://doi.org/10.3390/en15228655

Academic Editor: Adrián Mota Babiloni

Received: 28 September 2022
Accepted: 14 November 2022
Published: 18 November 2022

1. Introduction

Baking is one of the key processes that strongly affect the production yield, final price, and quality of tobacco leaves [1]. Currently, coal-fired bulk curing barn (TCCB) is China's most widely used tool for curing tobacco leaves [2–5]. This method requires a large air volume and the external drainage are remarkable. Although TCCB is low-price equipment and can be used for large-scale baking, the temperature fluctuation during the baking process can be hardly controlled, resulting in a low baking quality of the processed tobacco leaves. Moreover, some part of heat and humid gases are discharged from the curing barn, thereby reducing energy efficiency and resulting in environmental issues by exhausting coal-fired flue gases [6]. To solve the problem, numerous investigations have been carried out to achieve an even temperature distribution in the barn. In this regard, different algorithms and analytical methods have been proposed [7–10]. Recently, replacing coal with methanol and biomass has become a research hot spot [11–13]. Based on these methods, the temperature control accuracy has been improved and the flue gas emission has been reduced effectively. However, the curing cost is high and the thermal efficiency of the curing process should be further improved.

Studies show that heat pump drying technology is an effective scheme to resolve the problems of emission pollution and high energy consumption in curing barns. In this way, the moisture can be separated from the curing medium while the high-temperature dry medium is retained for internal recycling [14–16]. Subsequently, the energy waste and aroma volatilization caused by the drainage is reduced, thereby improving the quality of the cured tobacco leaves [17,18]. Recently, heat pump drying technology has been widely

used in processing agricultural products. Arley Salazar-Hincapié et al. [19] conducted an experimental study on Oregano heat pump drying, and studied the effects of variations in compressor discharge pressure on the COP value, drying kinetics, and the specific moisture extraction rate of Oregano. It was found that for the Oregano samples with the same initial moisture content, the lower the compressor discharge pressure, the lower the drying temperature, and the higher the quality of the dried Oregano. Ma X Z et al. [20] proposed a paddy grain heat pump dryer and investigated the exergetic performance of the dryer. The results showed that the proposed heat pump dryer outperforms the traditional hot air dryer in terms of energetic aspects. The COP value of the proposed heat pump and the corresponding specific energy consumption reached were 3.72 and 1925 kJ·kg^{-1} H_2O, respectively. Moreover, Li C Y et al. [21] conducted a comparative study between the energy performance of a paddy grain heat pump drying system and a traditional coal-fired hot air drying system and showed that the heat pump drying system improves energy efficiency and reduces heat losses. The performed analyses revealed that heat pump drying technology is an environment-friendly scheme with wide applications in processing agricultural products. Although this method has remarkable advantages such as low energy consumption, only a few works have been reported on the tobacco drying process.

To explore an energy-saving, environment-friendly, and high-quality tobacco leaf drying process, the present work adopted the widely used heat pump drying technology to dry the tobacco leaves. Moreover, a novel heat pump tobacco bulk curing barn (HPCB) was introduced. To comprehensively understand the drying performance of the HPCB, the temperature distribution, the dehumidification characteristics, quality of tobacco leaves, thermal efficiency, total energy consumption, and economic aspects of the HPCB were investigated numerically. Then, the main indicators of the HBCP were compared with that of the TCCB. This article is expected to provide a fundamental basis for designing the tobacco leave baking equipment and optimizing the tobacco leave drying process.

2. Materials and Methods

2.1. Materials

The experiment was conducted at Nanxiong Tobacco Research Institute, Shaoguan, Guangdong Province, China in July 2021. The tobacco species were selected from the central part of the flue-cured tobacco variety of Yueyan No. 97 in the same growth condition and maturity. It is worth noting that Yueyan No. 97 is a widely planted species of tobacco in the south of China. It has a high yield, good appearance, and high quality. This study is of significant importance because increasing the proportion of middle- and high-grade tobacco has huge economic benefits. The test curing barn consists of two air-falling-type bulk curing barns with the following specifications: the loading room ($L \times W \times H$) was 8.0 m × 2.7 m × 3.5 m and the total loading capacity was about 4300 kg. Tobacco leaves were used to hang tobacco in the upper, middle, and lower sheds as showed in Figure 1.

2.2. Equipment and Its Working Principle

Figure 1 shows the configuration of the experimental equipment, which is mainly composed of a bulk curing barn, temperature and humidity detection systems, a dehumidification system, and a smart control system. The bulk curing barn includes a fan, central ventilation system, air inlet, air outlet, and heating devices. In the present study, HPCB and TCCB devices were considered and compared. The main parameters of the heat pump are presented in Table 1.

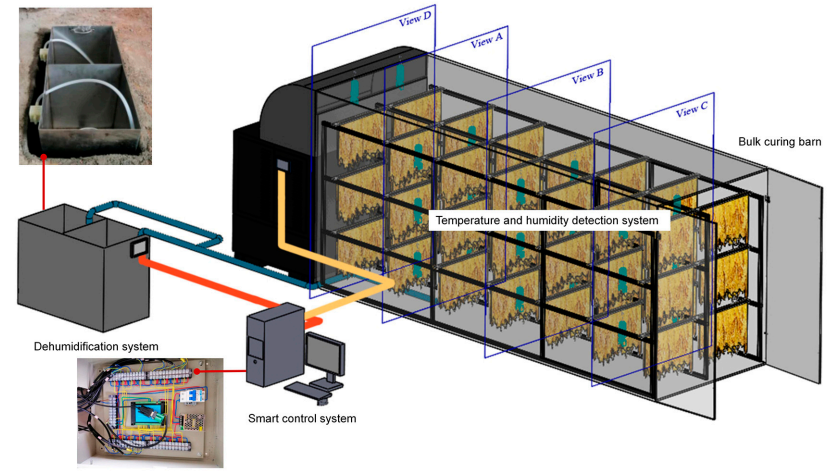

(**a**)

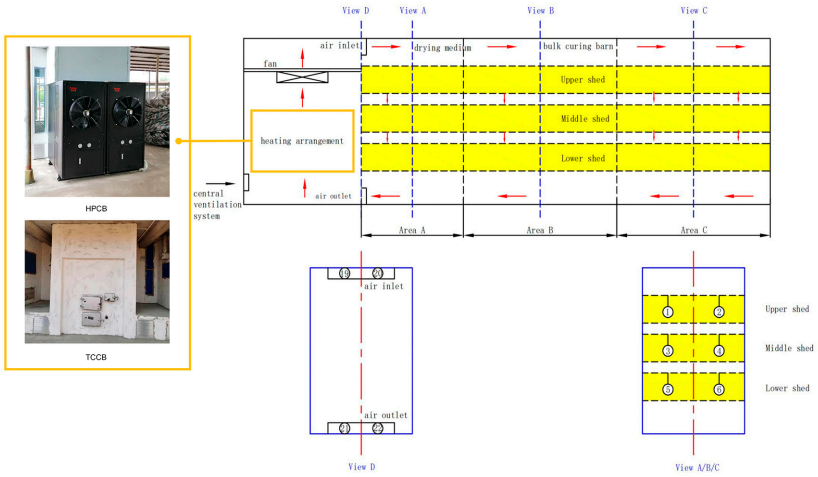

(**b**)

Figure 1. The experimental equipment: (**a**) structure and (**b**) schematic diagram of the bulk curing barn.

Table 1. The main parameters of the HPCB.

Model	Nominal Eating Capacity	Nominal Input Power	Electric Auxiliary Heat Power	Circulating Air Flow	Refrigerant
NHGCS-48S	34,836 W	11,642 W	12 kW	19,000 m^3/h	R134a
Pressure	Maximum drying temperature	Maximum dehumidification capacity	Maximum heating capacity	Maximum input power	Circulating fan
2.8 MPa	75 °C	50 kg/h	43,546 W	14,324 W	1.1 kw * 2

Figure 1b shows the working principle of HPCB and TCCB. When the fan and the heating device were operated, the system heated the air that passes the central ventilation system. Then the hot air flow was transferred to the bulk curing barn through the air inlet. In the curing barn, heat and mass exchange occurred between hot air and tobacco so the temperature of hot air decreased and its humidity increased, as shown by the red arrows in Figure 1b. After heat and mass exchange, the air flow returned to the heating arrangement system through the air outlet, where the air temperature increased and its

moisture decreased. Meanwhile, the condensed water in the pipe of the humidity detection system was discharged.

Since no hot air is vented from the bulk curing barn, the drying process is a closed system, so the thermal energy and aroma of tobacco circulate in the curing barn. Consequently, the energy efficiency of the system and the tobacco quality improve.

2.3. Testing Method

The experiment was carried out in an air-flow falling bulk curing barn. In this regard, temperature field tests, dehumidification tests, and energy efficiency tests were carried out on HPCB and TCCB systems, and the obtained results were compared. Furthermore, the effects of HPCB on the temperature distribution, dehumidification, and energy saving of flue-cured tobacco were analyzed.

2.3.1. Temperature Field Experiment

The length of the curing barn was 8 m, and plane D was the inlet and outlet air view. At 1 m, 3.5 m, and 6.5 m from the view D, views A, B, and C were selected, respectively. In the drying process, the heated air enters the curing barn and passes through the upper shed, middle shed, and lower shed tobacco. Finally, the air returns to the heating arrangement system. The process parameters are shown in Table 2.

Table 2. Parameters of the baking process.

Baking Stage	Dry-Bulb Temperature/°C	Wet-Bulb Temperature/°C	Time/h
Early-yellowing stage	38	36	24
Mid-yellowing stage	40	37	20
Late-yellowing stage	42	37.5	20
Early-fixing-color stage	46	37.5	21
Mid-fixing-color stage	50	38	24
Late-fixing-color stage	54	39	20
Early-stem-drying stage	60	40	10
Late-stem-drying stage	65–68	42–43	22

2.3.2. Energy Consumption Tests

The temperature and energy tests were designed to analyze the temperature change and perform energy analysis in the curing barn. Twenty-two points were considered in the bulk curing barn to measure dry-bulb and wet-bulb temperatures using a temperature sensor (Xi'an SENWAS company, DS18B20, Xi'an, China). The characteristics of the instrument are presented in Table 3. After calibrating the temperature sensors, they were installed in the curing barn as shown in Figure 1b. It is worth noting that there were two sensors in the input air and two sensors in the output air. Meanwhile, six sensors were installed in views A, B, and C. The data were recorded every 10 min in the smart control system. The average of six temperatures in an hour was taken as the temperature of the acquisition point. There was an electric meter (Zhuhai Pilot Technology Company, SPM93, Zhuhai, China) in the curing barn for automatic recording of the energy consumption data. The types and uncertainty of sensors are listed in Table 3.

Table 3. Types and uncertainty of the test instruments.

Instruments	Type	Uncertainty	Detection Range
Temperature sensor	DS18B20	±0.1 °C	−55 °C ~ +125 °C
Electric meter	SPM93	0.01 V/0.01 A/0.01 W	−99,999.99 ~ +99,999.99

2.3.3. Dehumidification Characteristics

In the present study, a self-developed humidity detection system shown in Figure 1a was used to measure humidity in the process. When the high-temperature and high-

humidity drying medium passed the heating arrangement, the temperature and humidity of the drying medium continuously reduced through the bulk curing barn. Meanwhile, the condensed water was discharged from the heating arrangement system and flowed into the humidity detection system, where the dehumidification capacity was calculated in the control system. The dehumidification capacity was measured once every 30 min, and the hourly capacity was calculated accordingly.

2.4. Evaluation Methods and Models

2.4.1. The Regional Temperature Eigenvalue

The regional temperature eigenvalue of the curing barn area was defined as a measure of the temperature of each distribution area. The mathematical expression in Equation (1) indicates, in this parameter, the regional block volume with the temperature acquisition point identified in Table 4. The regional temperature eigenvalue can be obtained by integral conversion of temperature and volume over all blocks in the region.

$$T_a = \frac{1}{V} \cdot \int\int\int T dx dy dz \quad (1)$$

where T_a is the regional temperature eigenvalue, °C; T is the temperature of the temperature acquisition point in the region, °C; $dxdydz$ represents the volume of the area where the temperature acquisition points are located, m^3; and V is the volume of the region, m^3.

Table 4. Region volume of each temperature acquisition point.

Region	Temperature Acquisition Point	Region Volume (dx × dy × dz)
A	1–6	2.0 m × 1.35 m × 1 m = 2.7 m^3
B	7–12	3.0 m × 1.35 m × 1 m = 4.05 m^3
C	13–18	3.0 m × 1.35 m × 1 m = 4.05 m^3

Figure 1 and Table 4 indicate that the regional volume of view A was 2.7 m^3, and the regional volume of views B and C were 4.05 m^3.

2.4.2. Uniformity of the Regional Temperature Filed

The uniformity of the regional temperature field is defined as the maximum difference between the temperature of the regional temperature acquisition point in the curing barn and the eigenvalues of the regional temperature in a stable temperature state. This can be mathematically expressed as follows:

$$\Delta T = T_{amax} - T_{amin} + 0.55 \cdot (\sigma_{max} - \sigma_{min}) \quad (2)$$

where ΔT is the uniformity of the temperature field in the region, °C; T_{amax} and T_{amin} are the maximum and minimum temperature eigenvalues in the region, respectively; σ_{max} and σ_{min} are the standard deviation of the maximum and minimum temperature eigenvalues, respectively, °C. It is worth noting that the smaller the uniformity, the more stable the temperature field in the studied region.

2.4.3. The Temperature Charts along the Horizontal Direction

Uniformity of the temperature distribution is an important parameter in the tobacco bulk curing barn [22]. HPCB or TCCB systems have different heating arrangements in heating the bulk curing barn, thereby resulting in different heat waving characteristics in the distinct heating arrangement. The temperature distribution in the curing barn was maintained at a fixed value by intermittent operation of the heating arrangement in the drying process. When the temperature fell lower than the pre-set value, the system was

turned on, and then it was turned off once the temperature reached the preset high value. The energy demands and supplying models are as follows:

$$Q_{demands} = c_{total} m \Delta T \tag{3}$$

$$Q_{supplying} = P_{TCCB} \cdot t \tag{4}$$

$$Q_{supplying} = \int_0^t P_{HPCB}(t) \cdot dt \tag{5}$$

where $Q_{demands}$ is the energy demands of bulk curing barn, J; c_{total} is the specific heat capacity of the substance, J/kg·°C; ΔT is the temperature gradient, °C; $Q_{supplying}$ is the heating arrangement creating energy, J; P_{TCCB} is the power of TCCB, W; P_{HPCB} is the power of HPCB, W; and t is drying time, s.

Equation (3) indicates that the energy demands $Q_{demands}$ for each room temperature jumping is affected by the specific heat capacity (c_{total}) of substance in the bulk curing barn, the mass of the heated substance (m), and the temperature gradient (ΔT). Then the heating arrangement should support energy $Q_{supplying}$, which is higher than energy demands $Q_{supplying}$. There is an advanced electronic control system in HPCB, which can control energy output much more precisely than TCCB does, which uses an air input control device. Theoretically, the HPCB system can control the temperature of the drying room more homogeneously and efficiently than the TCCB does.

2.4.4. The Dehumidification Capacity and Efficiency

The dehumidification capacity per hour can be obtained through the dehumidification capacity acquisition system. Then the dehumidification efficiency can be calculated using the following expression:

$$\eta_W = \frac{W_n}{n \cdot \sum W_n} \times 100\%, (n = 1, 2, 3, 4 \cdots) \tag{6}$$

2.4.5. Thermal Efficiency of the Curing Barn

Based on the consumption of coal and electricity in the TCCB and HPCB systems, the total energy consumption of the drying process and the curing cost per kg of dry tobacco can be calculated. Combined with the quality of fresh and dried tobacco leaves, the actual amount of water removed from the tobacco leaves can be calculated. Accordingly, the energy consumption of the curing barn can be calculated under the assumption that both curing barns have the same heat dissipation. Then the thermal efficiency of TCCB and HPCB systems can be calculated using the following expressions [23]:

$$\eta_{TC} = \frac{E_{exergy}}{E_{energy.TC}} \times 100\% = \frac{\sum_{i=1}^{n} h_{fgi} \cdot m_{wi}}{m_{TC} \cdot q_1 + Q_{TC} \cdot q_2} \times 100\% \tag{7}$$

$$\eta_{HP} = \frac{E_{exergy}}{E_{energy.HP}} \times 100\% = \frac{\sum_{i=1}^{n} h_{fgi} \cdot m_{wi}}{Q_{HP} \cdot q_2 \cdot COP} \times 100\% \tag{8}$$

$$h_{fgi} = 2.503 \times 10^6 - 2.386 \times 10^3 \cdot (T_i - 273.16) \quad 273.16 \le T_i \le 338.72 \tag{9}$$

$$h_{fgi} = \left(7.33 \times 10^{12} - 1.60 \times 10^7 \cdot {T_i}^2\right)^{0.5} \quad 338.72 \le T_i \le 533.16 \tag{10}$$

where η is the thermal efficiency of the curing barn, %, E_{exergy} is the useful energy for the energy consumption of the oven, kJ; $E_{energy,TC}$ is the total energy consumption of TCCB, including coal and electricity consumptions, kJ; h_{fg} is the latent heat, J/kg; m_{wi} is the actual amount of water removed per unit time from tobacco leaves, kg; q_1 is the low calorific value of standard coal, which is 29,295 kJ/kg; Q_{TC} is the power consumption of TCCB, kWh; q_2 is the conversion coefficient of electric energy and heat energy, which is 3600 kJ/kWh; $E_{energy,HP}$ is the total energy consumption of HP curing barn, kJ; Q_{HP} is the

power consumption of HPCB, kWh; *COP* is the cycle performance coefficient of the heat pump. In this study, *COP* = 2.5.

3. Results and Discussions

3.1. The Analysis of Temperature Eigenvalue for TCCB and HPCB Systems

In order to investigate the influence of TCCB and HPCB systems on the temperature distribution in the bulk curing barn, the temperature data measured at the acquisition points were compared with the set process curve, and the deviation values were analyzed by SPSS software. The obtained results are presented in Figure 2 and Table 5.

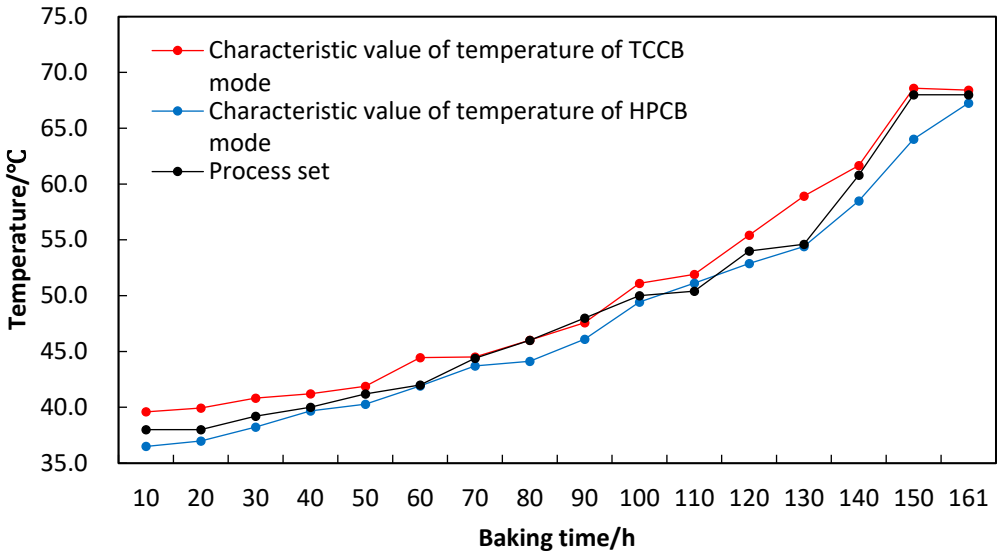

Figure 2. Temperature value of the TCCB and HPCB systems.

Table 5. Analysis of variance between TCCB and HPCB and process set curve.

Baking Mode	Maximum Deviation/°C	Mean Deviation/°C	Variance Deviation/°C	Standard Deviation Deviation/°C
TCCB	4.32	1.268	1.122	1.059
HPCB	3.97	1.183	0.949	0.974

Figure 2 shows that the temperature eigenvalue of TCCB and HPCB gradually increased with the curing time, and the development was consistent with the set process curve. Table 5 indicates that the maximum deviation between TCCB and the set process was 4.32 °C, the mean deviation was 1.268 °C, the variance was 1.122 °C, and the standard deviation was 1.059 °C; Moreover, the maximum deviation between HPCB and the set process was 3.97 °C, the deviation mean was 1.183 °C, the variance was 0.949 °C, and the standard deviation was 0.974 °C. The results showed that the temperature fluctuation in the HPCB system was less than that of the TCCB system, indicating that the HPCB system could provide a more stable temperature field for tobacco curing. It should be indicated that the smaller the temperature fluctuation, the smaller the loss of the tobacco substance, and the higher the final quality of the curing tobacco [5].

3.2. The Temperature Field Uniformity Analysis of TCCB and HPCB along the Horizontal Direction

The spatial distribution of temperature is of significant importance in tobacco curing. During the experiment, acquisition points 1, 2, 7, 8, 13, and 14 were selected to represent the upper shed area, and acquisition points 5, 6, 11, 12, 17, and 18 were selected to represent the lower shed area. The temperature eigenvalue, standard deviations, and temperature uniformity of the upper and lower shed areas along the horizontal direction

can be calculated by substituting the temperature data of the above 12 acquisition points into Equations (1) and (2). The onset of yellowing temperature, the transition temperature from the yellowing stage to the color-fixing stage, and the temperature for the main veins of tobacco to turn brown were 38 °C, 42 °C, and 50 °C, respectively. Moreover, the drying temperature of the main veins in the stem-drying stage was 68 °C. The temperature uniformity along the horizontal direction of TCCB and HPCB is presented in Figures 3 and 4.

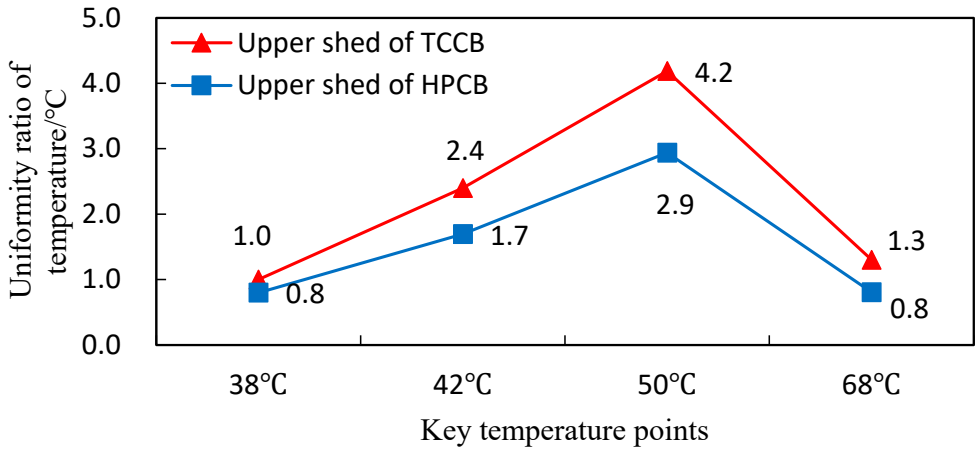

Figure 3. The uniformity ratio of upper shed temperature in TCCB and HPCB modes along the horizontal direction.

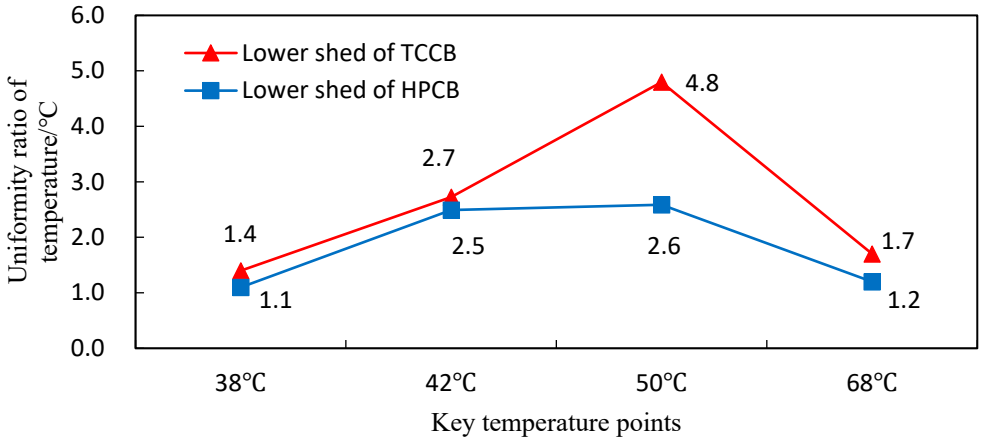

Figure 4. The uniformity ratio of lower shed temperature in TCCB and HPCB modes along the horizontal direction.

Figures 3 and 4 show that at the four temperature states, the uniformity of the upper and lower sheds of TCCB along the horizontal direction was greater than that of HPCB, and the maximum uniformity occurred at 50 °C. In the upper shed, the maximum uniformity of TCCB was 4.2 °C and the maximum uniformity of HPCB was 2.9 °C; in the lower shed, the maximum uniformity of TCCB was 4.8 °C and the maximum uniformity of HPCB was 2.6 °C. Chen J L [23] demonstrated that in the chrysanthemum heat pump drying process, the smaller the uniformity, the more stable the regional temperature field. The obtained results revealed that uniformity of HPCB is smaller than that of TCCB, indicating that HPCB provides a uniform temperature field in the curing process so tobacco leaves are cured at a stable condition, thereby improving the curing quality.

3.3. Analysis of Temperature Field Charts in TCCB and HPCB Modes along the Horizontal Direction

According to the temperature eigenvalue of each temperature point obtained from the test data, acquisition points 1, 2, 7, 8, 13, and 14 were selected to represent the upper shed

area, while acquisition points 3, 4, 9, 10, 15, and 16 were selected to represent the middle shed area, and the collection points 5, 6, 11, 12, 17, and 18 were selected to represent the lower shed area. Meanwhile, the four temperatures of 38, 42, 50, and 68 °C were selected as the temperature observation points. The temperature charts were drawn using MATLAB software and the horizontal temperature variation TCCB and HPCB at four key temperature points were analyzed accordingly. The obtained results are shown in Figures 5–8.

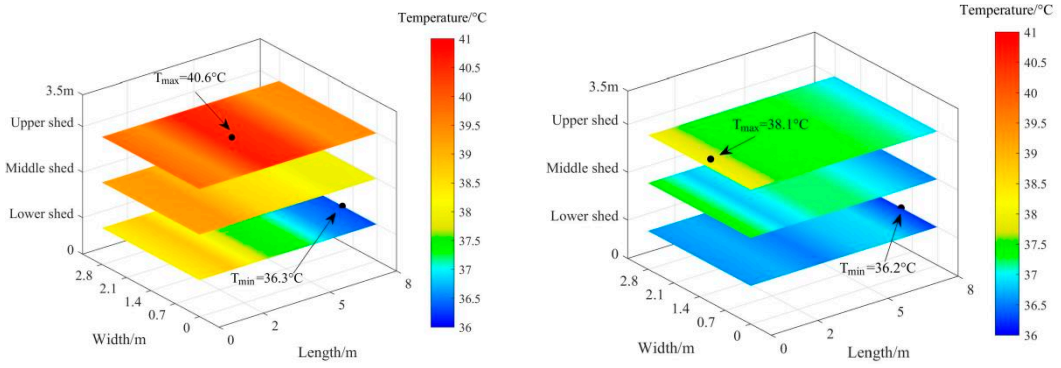

(**a**) (**b**)

Figure 5. The temperature distribution of (**a**) TCCB and (**b**) HPCB with a curing temperature of 38 °C.

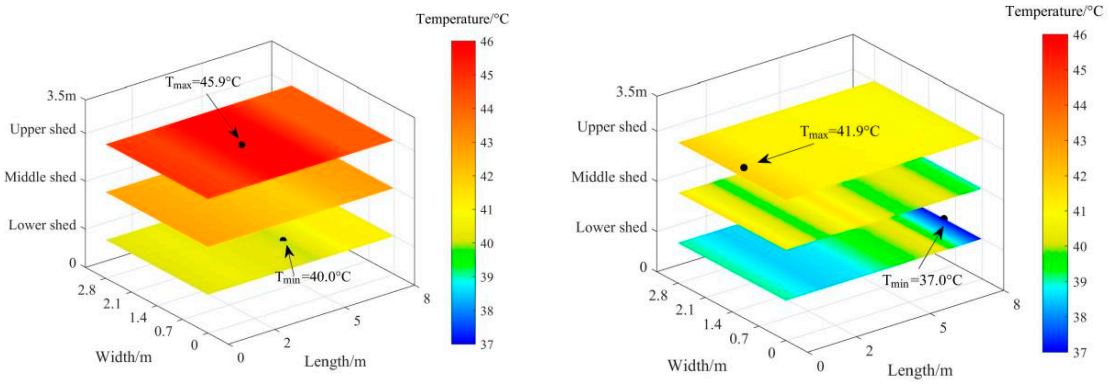

(**a**) (**b**)

Figure 6. The temperature distribution of (**a**) TCCB and (**b**) HPCB with a curing temperature of 42 °C.

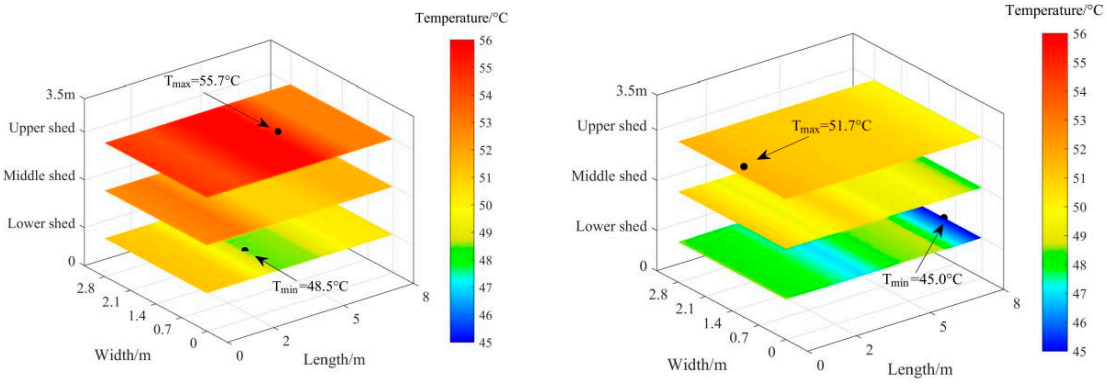

(**a**) (**b**)

Figure 7. The temperature distribution of (**a**) TCCB and (**b**) HPCB with a curing temperature of 50 °C.

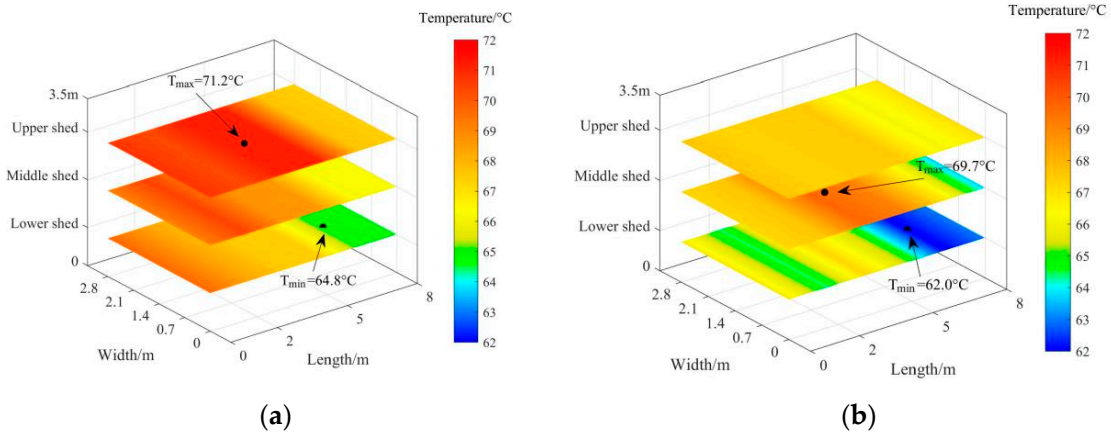

Figure 8. The temperature distribution of (**a**) TCCB and (**b**) HPCB with a curing temperature of 68 °C.

Figure 5 indicates that when the curing temperature was 38 °C, the tobacco leaves were in the early yellowing stage, and the temperature of tobacco leaves changes in the range of 36–41 °C. Moreover, it was found that the highest and the lowest temperature of TCCB was 40.6 °C and 36.3 °C, located in the middle region of the upper shed cross-section and in the rear region of the lower shed cross-section, respectively; the highest and the lowest temperature of HPCB was 38.1 °C and 36.2 °C, occurring in the front end of the upper shed cross-section and in the rear end of the lower shed cross-section, respectively. Figure 5 shows that the variation range of temperature in TCCB was 4.3 °C, while it was only 1.9 °C in HPCB, indicating that the temperature field was more uniform in HPCB. This is consistent with the results of Persimmon slices heat pump drying reported by Tang, X.X. et al. [24]. The temperature distributions of the upper shed and middle shed cross-sections in TCCB were uniform, while the stratification of the lower shed cross-section was obvious, and the temperature distribution range was 36.3–38 °C. It was found that the temperature near the return outlet was high, while the temperature near the back end was low. The temperature distributions of the upper shed, middle shed, and lower shed cross-sections in HPCB were relatively uniform, and the temperature of the upper shed was large. This is because the bulk curing barn located in the front end of the upper shed is an air inlet, in which the temperature gradient is small and the temperature stratification decreases slowly from the upper shed to the lower shed.

Figure 6 shows that when the temperature of flue-cured tobacco was 42 °C, the tobacco leaves were in the late yellowing stage to the early color-fixing stage, and the temperature range was 37–46 °C. Under these conditions, the highest and lowest temperature of TCCB, which occurred in the middle area of the upper and lower shed cross-sections, reached 45.9 °C and 40.0 °C, respectively. Furthermore, the maximum and minimum temperature of HPCB, which occurred in the front end and back end of the upper and lower shed cross-sections, reached 41.9 °C and 37.0 °C, respectively. Figure 6 reveals that the temperature range of TCCB was 5.9 °C, which is slightly higher than 4.9 °C for HPCB, indicating that the temperature field distribution uniformity of HPCB was slightly higher than that of TCCB. In TCCB, the temperature distributions of the upper shed, middle shed, and lower shed cross-sections were relatively uniform in each layer. The overall temperature of the upper shed was higher, followed by the middle shed, and the lower shed had the lowest temperature. In the HPCB mode, the temperature distributions of the upper shed and the middle shed cross-sections were relatively uniform in each layer. The temperature stratification of the lower shed cross-section varied in the range of 37.0–41.0 °C. The temperature near the return air outlet was high, while there was a low-temperature zone near the back end.

Figure 7 reveals that when the temperature of flue-cured tobacco was 50 °C, the tobacco leaves were in the middle and late stage of color-fixing, and the temperature varied in the range of 45–56 °C. The highest temperature of TCCB reached 55.7 °C, which occurred in the middle area of the upper shed cross-section and the lowest temperature was 48.5 °C,

which was located in the middle area of the lower shed cross-section. The maximum and minimum temperatures of HPCB, which occured in the front end of the upper shed cross-section and the back end of the lower shed cross-section, were 51.7 °C and 45 °C, respectively. Figure 7 indicates that the temperature fluctuations of TCCB and HPCB were consistent. The temperature range of TCCB was 7.2 °C, while that of HPCB was 6.7 °C. In TCCB, the temperature distribution of the upper, middle, and lower shed cross-sections were relatively uniform in each layer. The highest temperature occurred in the upper shed, followed by the middle shed, and the lowest occurred in the lower shed. In HPCB, the temperature distributions of the upper and middle shed cross-sections were relatively uniform in each layer. The temperature stratification of the lower shed cross-section was 45–48 °C, in which high-temperature and low-temperature zones occured near the return air outlet and the back end, respectively.

Figure 8 shows that when the temperature of flue-cured tobacco reached 68 °C, the tobacco leaves were in the late stage of stem-drying and the temperature range was 62–72 °C. The highest temperature of TCCB reached 71.2 °C, which occurred in the middle area of the upper shed cross-section and the lowest temperature was 64.8 °C, which occurred in the back end of the lower shed cross-section. Moreover, it was found that the maximum and minimum temperatures of HPCB reached 69.7 °C and 62.0 °C, which occurred in the front end and back end of the upper and lower shed cross-section, respectively. Figure 8 shows that the temperature fluctuation of TCCB was 6.4 °C, which is slightly higher than 5.7 °C for HPCB. In TCCB, the temperature distributions of the upper and middle shed cross-sections were relatively uniform in each layer, while the temperature of the lower shed cross-section was lower and varied in the range of 64.8–68 °C. Sun L [25] demonstrated that this distribution meets the requirements of curing tobacco leaves during the stem-drying stage. In HPCB, the temperature distributions of upper and middle shed cross-sections in each layer were relatively uniform and the overall temperature distribution met the requirements of curing tobacco leaves in the stem-drying stage.

According to the temperature field charts of TCCB and HPCB in the horizontal direction, the maximum temperature of TCCB was higher than that of HPCB with a relatively uniform temperature distribution in each shed. However, at some key temperature points, the temperature of the lower shed was low and stratified. This was especially more pronounced in the back end of the lower shed. In general, HPCB can effectively form a stable temperature flow field in the curing barn and significantly improve the curing quality of tobacco leaves.

3.4. Analyzing the Dehumidification Capacity of the Heat Pump

During the experiment, the dehumidification capacity at each stage of tobacco curing was measured by the humidity detection system. Then, the dehumidification efficiency at each stage was calculated by Equation (6). The results are presented in Table 6.

Table 6. The dehumidification capacity and efficiency in baking stages.

Baking Stage	Baking Time/h	Dehumidification Capacity *W*/kg	Mean Dehumidification Capacity W_n kg/h	Dehumidification Efficiency η_w%/h
Early-yellowing stage	24	342.96	14.29	0.40
Mid-yellowing stage	20	410.60	20.53	0.57
Late-yellowing stage	20	505.60	25.28	0.70
Early-fixing-color stage	21	665.07	31.67	0.88
Mid-fixing-color stage	24	780.24	32.51	0.91
Late-fixing-color stage	20	612.40	30.62	0.85
Early-stem-dring stage	10	205.90	20.59	0.57
Late-stem-dring stage	22	68.64	3.12	0.09
Total	161	3591.41	22.31	-

Table 6 indicates that the temperature of the drying medium gradually increased in the barn. Moreover, mean dehumidification capacity W_n and dehumidification efficiency η_w increased first and then decreased, which can be interpreted by water loss of tobacco leaves in the drying process. During the experiment, the maximum and minimum W_n were 32.51 kg/h and 3.12 kg/h, respectively, and the total W was 3591.41 kg. In the yellowing stage, the temperature of the drying medium of tobacco leaves was low, the moisture of fresh tobacco leaves was high, and the relative humidity of the tobacco loading chamber was high. Moreover, the total W was 1259.16 kg (342.96 + 410.60 + 505.60), accounting for 35.06% of the total W of the whole process. When leaves entered the color-fixing stage, the water loss of tobacco leaves accelerated and the dehumidification capacity and efficiency improved significantly. The maximum dehumidification capacity reached 32.51 kg/h, and the dehumidification efficiency exceeded 0.85%/h, indicating that the dehumidification efficiency was high. During the color-fixing stage, the total dehumidification capacity was 2057.71 kg (665.07 + 780.24 + 612.40), accounting for 57.3% of the total dehumidification in the drying process. In the stem-drying stage, most of the initial moisture was discharged and a little amount of moisture remained in the veins of leaves. Accordingly, the water loss rate after this stage was low. Subsequently, the dehumidification capacity was low (3.12 kg/h) and the dehumidification efficiency dropped significantly and reached 0.09%/h. The total dehumidification capacity in the drying period was 274.54 kg (205.90 + 68.64), accounting for 7.64% of the total dehumidification capacity. Furthermore, the total dehumidification capacity during the stem-drying stage was 274.54 kg, accounting for 7.64% of the total dehumidification.

The HPCB is an effective scheme to resolve the problems of high energy consumption in curing barns by recycling the energy with the condensate water (dehumidification capacity). The more the condensate water is discharged from the system, the more energy will be recycled and then return to the heating arrangement system again.

3.5. The Appearance Quality Evaluation of Tobacco after Curing

The visual quality of tobacco after curing by TCCB and HPCB is shown in Table 7 and Figure 9. It was observed that there were certain differences in the appearance quality of the two process modes. The differences were in color, structure, green degree, and ash content, while there were no obvious differences in other indicators such as maturity, oil content, identity, and chrominance. The appearance of curing tobacco with TCCB was mature with high oil content, orange-lemon color, medium identity, compact structure, strong chrominance, and a certain degree of green and hanging ash. The appearance of curing tobacco with HPCB was mature with high oil content, orange color, medium identity, loose structure, strong chrominance, slightly green, and low ash content. The HPCB's performance was slightly better than that of the TCCB in color, structure, green degree, and ash content.

Table 7. Quality evaluation of the tobacco appearance after curing.

Curing Mode	Maturity	Oil Content	Color	Identity	Structure	Chroma	Contain Green Degree	Hanging Ash
TCCB	mature	multiple	orange-lemon	middle	compact	strong	find	find
HPCB	mature	multiple	orange-yellow	middle	rarefaction	strong	slightly	micro

Note: The red text marks the better qualities.

(**a**) (**b**)

Figure 9. Appearance of tobacco leaves after curing with (**a**) TCCB and (**b**) HPCB modes.

3.6. Evaluation of Chemical Properties of Tobacco after Curing

The chemical properties of tobacco leaves after curing with TCCB and HPCB are shown in Table 8. It should be indicated that in high-quality tobacco, the ratio of the reduced sugar to the total sugar should be ≥ 0.9, the ratio of the reduced sugar to nicotine should be in the range of 8–12, the total nitrogen/nicotine should be less than 1, and the ratio of potassium to chloride should be greater than 4. Table 5 shows that the ratio of the reduced sugar to the total sugar in both TCCB and HPCB modes was greater than 0.9, and the potassium-to-chloride ratio was higher than 4. However, the reduced sugar/nicotine and the ratio of nitrogen to nicotine of HPCB were better than those of TCCB indicating that the main chemical components of HPCB have good coordination.

3.7. The Energy Efficiency and Economic Analysis of Bulk Curing Barn

During the curing process, the coal consumption, electricity consumption, and labor costs of TCCB and HPCB were recorded. In this regard, Table 9 shows that the mass of fresh tobacco, dry tobacco, and water removal in TCCB was 4376, 660.9, and 3715.1 kg, respectively. The coal consumption was 1.13 tons, and the power consumption of TCCB is 350 kWh. The total energy consumption cost was 1492 CNY and the labor cost was about 270 CNY, so the total cost was 1762 CNY, and the cost per unit mass of dry tobacco was 2.67 CNY/kg. Moreover, the mass of fresh tobacco, dry tobacco, and water removal in HPCB was 4221, 629.59, and 3591.41 kg, respectively. The power consumption of HPCB was about 1420 kWh. The total energy consumption cost was 781 CNY and the labor cost was 54 CNY, so the total cost was 835 CNY and the cost per unit mass of the dry tobacco was 1.34 CNY/kg. It is found that the unit cost of HPCB was only 50.19% that of TCCB.

The thermal efficiency of the curing barn can be calculated by substituting the data of Table 9 into Equations (7) and (8). The obtained results in Table 10 show that the exergy value of TCCB was 9,622,109 kJ, the coal energy consumption was 21,636,176.47 kJ, and the electricity consumption was 1,260,000 kJ. Accordingly, the total energy consumption was 22,896,176.47 kJ, and the thermal efficiency was 42.02%. Similarly, the energy value of HPCB was 8,598,387 kJ, the total energy consumption was 12,924,000 kJ, and the thermal efficiency was 66.53%. Accordingly, the thermal efficiency of HPCB was obviously higher than that of TCCB.

The performed analyses demonstrated that, compared with TCCB, with a thermal efficiency of 42.02%, the thermal efficiency of HPCB reached 66.53%. This remarkable difference originates from different structures of HPCB and TCCB, and energy saving in the HPCB mode. For TCCB, the heat loss includes the hot flue tail gas and the hot air that is discharged from the curing barn, which causes huge energy waste and may even lead to environmental issues. There is no hot air vent in HPCB and energy is recovered in the whole process. Compared with the TCCB, HPCB has higher energy efficiency and lower waste of energy.

Table 8. The chemical composition of tobacco leaves after curing.

Curing Mode	Total Sugar/%	Reducing Sugar/%	Total Nicotine/%	Total Nitrogen/%	Chlorine/%	Potassium/%	Reducing Sugar/Total Sugar	Reducing Sugar/nicotine	Total Nitrogen/Nicotine	The Potassium-to-Chloride Ratio/%
TCCB	28.7	27.5	1.66	2.05	0.10	2.38	0.96	16.57	1.23	23.80
HPCB	27.8	26.7	2.11	1.96	0.15	2.25	0.96	12.65	0.93	15.00

Notes: The red mark is the better one.

Table 9. Costs for the whole process of the two modes.

Baking Mode	Quality of Fresh Tobacco/kg	Quality of Dry Tobacco/kg	Dehumidification Capacity/kg	Coal Consumption/t	Electricity Consumption/kW	Total Energy Cost [(i)]/CNY	Human Cost [(ii)]/CNY	Total Cost/CNY	Unit Cost/CNY kg^{-1}
TCCB	4376	660.9	3715.1	1.13	350	1492	270	1762	2.67
HPCB	4221	629.59	3591.41	0	1436	789.8	54	843.8	1.34

Notes: [(i)] According to the local price, the coal price is 1150 CNY/ton, and the electricity price is 0.55 CNY/kWh; [(ii)] TC has 1.5 labor days, while HPCB has 0.3 labor days, curing technician labor costs is assumed to be 180 CNY per working day.

Table 10. The thermal efficiency of bulk curing barn.

Baking Mode	Exergy E_{exergy}/kJ	Coal Energy $m_{TC} \cdot q_1$/kJ	Electricity Energy $Q_{TC/HP} \cdot q_2$/kJ	Total Energy E_{energy}/kJ	Thermal Efficiency φ/%
TCCB	9,622,109	21,636,176.47	1,260,000	22,896,176.47	42.02
HPCB	8,598,387	0	12,924,000	12,924,000	66.53

4. Conclusions

In the present study, the temperature field of the tobacco curing barn with HPCB and TCCB systems was studied and energy analysis was carried out to compare the performance and quality of the final products of the two systems. To this end, the temperature field distribution, the economic issues, and the energy performance of HPCB and TCCB systems were investigated. The obtained temperature uniformity curves and analyzing different temperature key points confirmed that the HPCB could effectively provide a uniform and stable temperature field in the curing process. It was found that HPCB outperformed TCCB in terms of appearance quality measures such as color, structure, green degree, and ash content. The unit dry tobacco cost of HPCB was only 50.19% of that of TCCB. The performed analyses demonstrated that the thermal efficiency of HPCB (66.53%) was significantly higher than that of TCCB (42.02%). This article is expected to provide a reference for designing the tobacco leaf heating equipment and optimizing the drying process.

Author Contributions: Conceptualization, Y.Z., C.L.; data curation, Y.Z., X.Z.; formal analysis, Y.Z., W.O., B.L., M.M.; funding acquisition, Y.Z., Z.H.; investigation, B.L., J.Z.; methodology, B.L., J.Z., X.Z.; software, W.O.; supervision, C.L.; writing—original draft, Y.Z., B.L. All authors have read and agreed to the published version of the manuscript.

Funding: This work was supported by the National Natural Science Foundation of China (No. 32171906; 31671783) and Science and Technology Project of Guangdong Tobacco Monopoly Bureau (№: yueyankexiang 202105).

Data Availability Statement: Not applicable.

Acknowledgments: The authors would like to thank the editors and reviewers for their valuable and constructive comments.

Conflicts of Interest: The authors declare that we have no known competing financial interests or personal relationships that could have appeared to influence the work reported in this paper.

References

1. Sun, X.H.; Zhao, L.; Wang, Y.P. Status quo and development trend of smokeless tobacco products. *Tob. Sci. Technol.* **2015**, *48*, 83–90. [CrossRef]
2. Dou, Y.; Shen, Y.; Yang, J. The development and prospect of novel tobacco products. *Chin. Tob. Sci.* **2016**, *37*, 92–97. [CrossRef]
3. Du, K.; Sun, B.; Cheng, W.; Zhang, Y. Design Method of Cam for Tobacco Rods Separating Drum in PROTOS2-2 Cigarette Maker. *Tob. Sci. Technol.* **2014**, *5*, 27–29. [CrossRef]
4. Ren, J.; Sun, F.S.; Liu, Z.Q.; Xu, S.F.; Xu, J.S.; Shen, S.Q. Development of bulk curing barns with central hot water heating system fueled by liquefied natural gas(LNG). *Acta Table Sin.* **2013**, *19*, 35–40. [CrossRef]
5. Ren, J.; Bai, R.; Yuan, W. Effects of Bulk Curing with Central Hot Water Heating System Fueled by Liquefied Natural Gas. *Chin. Tob. Sci.* **2014**, *35*, 89–92. [CrossRef]
6. Sun, X.J.; Du, C.Y.; Wang, Z.Q. Investigation into the design and development of heat pump equipped tobacco leaf bulk curing-barn. *Acta Table Sin.* **2010**, *16*, 31–35. [CrossRef]
7. Wen, J.; Wan, X.; Yang, Q. The Optimizing Combinative Test of Stable Time of Key Temperatures and Humidity Control during Bulk Curing Process. *Chin. Tob. Sci.* **2013**, *34*, 85–88. [CrossRef]
8. He, Q.X.; Liu, K.; Li, P. Time and Space Distribution of Temperature and Humidity and Differentiation of Interlayer Flue-Curing Effects during Curing in Bulk Curing Barn. *Shandong Agric. Sci.* **2017**, *49*, 54–59. [CrossRef]
9. Olejnik, T.P.; Mysakowski, T.; Tomtas, P.; Mostowski, R. Optimization of the Beef Drying Process in a Heat Pump Chamber Dryer. *Energies* **2021**, *14*, 4927. [CrossRef]
10. Zhao, H.B.; Wu, K.; Zhang, J.F. Simulation Study on Active Air Flow Distribution Characteristics of Closed Heat Pump Drying System with Waste Heat Recovery. *Energies* **2021**, *14*, 6358. [CrossRef]
11. Chen, Y.J.; Zhao, Z.X.; Zhu, L.C. Study on Effects of Tobacco Leaves Flue-Cured by Alcohol-based Fuel and Biomass Pellets. *Southwest China J. Agric. Sci.* **2019**, *32*, 1560–1565. [CrossRef]
12. Zhang, Y.W.; Yi, Z.X.; Zhou, Q.M. Effect of different bulk curing barns on baking energy consumption costs and upper leaves quality of flue-cured tobacco. *J. Gansu Agric. Univ.* **2019**, *54*, 112–120. [CrossRef]
13. Xu, X.X.; Chen, C.L.; Lv, Z.X. Study on Several New Type Bulk Curing Barns and Their Curing Effects. *Acta Table Sin.* **2017**, *38*, 82–86. [CrossRef]
14. Li, G.L.; Han, L.C.; Zhang, Z.Y.; Wang, G.H.; Jin, T.X.; Chen, G. Effect of Pretreatment on Drying Quality of Pitaya by Heat Pump. *Packaging Engineering.* **2022**, *15*, 105–113. [CrossRef]

15. Ba, Y. Uniform Air Supply and Heat Pump System Research in Closed Cycle Tobacco Baking Barn. Master's Thesis, Dalian University of Technology, Dalian, China, 2015.
16. Xue, T. Study on the Performance of an Air-Cooled Gravity Heat Pipe Dehumidification System in the Fully Closed Hot Air Circulating Bulk Curing Barn. Master's Thesis, Kunming University of Science and Technology, Kunming, China, 2018.
17. Ren, J.; Cao, Y.F.; Lu, X.H. Design and application of closed-loop heat pump curing barn with variable airflow direction. *Tob. Sci. Technol.* **2019**, *52*, 82–88. [CrossRef]
18. Lv, J.; Wei, J.; Zhang, Z.T. Experimental study on performance of heat pump system for tobacco leaf flue-curing. *Trans. Chin. Soc. Agric.* **2012**, *28*, 63–67. [CrossRef]
19. Salazar-Hincapié, A.; Delgado-Mejía, A.; Romero-Maya, A.F.; Duque-Grisales, E. Experimental Assessment of the Thermal Performance of a Heat Pump Dryer System Based on the Variations in Compressor Discharge Pressure on Oregano Drying. *Energies* **2020**, *13*, 6333. [CrossRef]
20. Ma, X.Z.; Fang, Z.D.; Li, C.Y. Energy efficiency evaluation and experiment on grain counter-flow drying system based on exergy analysis. *Trans. Chin. Soc. Agric. Eng.* **2017**, *33*, 285–291. [CrossRef]
21. Li, C.Y. *Engineering Thermodynamics and Heat Transfer*; China Agricultural University Press: Beijing, China, 2012. (In Chinese)
22. Chen, J.L. *Flow Field Analysis and Optimization Design of Air Source Heat Pump Chrysanthemum Drying Chamber*; Anhui University of Science Technology: Huainan, China, 2021. [CrossRef]
23. Gong, C.R. *Intensive Baking*; China Light Industry Press: Beijing, China, 2007.
24. Tang, X.X.; Zheng, J.; Ren, A.Q.; Duan, Z.H. Effects of heat pump drying temperature on drying characteristics and quality of persimmon slices. *Food Mach.* **2022**, *38*, 141–145, 216. [CrossRef]
25. Sun, L. Numerical Simulation and Experimental Analysis of Tobacco Drying in Dense Curing Barn with Variable Porosity Based on Water Transfer Model. Master's Thesis, Kunming University of Science and Technology, Kunming, China, 2021. [CrossRef]